25th ABCM International Congress of Mechanical Engineering
October 20-25, 2019, Uberlândia, MG, Brazil

COB-2019-2433
THEORETICAL STUDY OF THE THERMAL CONTACT RESISTANCE AS A FUNCTION OF SURFACE ROUGHNESS, MICROHARDNESS AND MOUNTING PRESSURE.

Daniel Dias Mendes
Joao Manoel Dias Pimenta
University of Brasilia - Department of Mechanical Engineering
danieldm1992@gmail.com
pimenta@unb.br

Abstract. *This paper presents the application of a mathematical model for the prediction of the thermal contact resistance between two dissimilar surfaces. A brief bibliographic review was performed on the subject, presenting the evolution of research over time, and an overview of the theoretical concepts involved. The theoretical development was thoroughly studied and summarised with as much as a concise explanation as possible. Numerical simulations were performed to observe the behaviour of thermal resistance occurring in the interface the surfaces for different mounting pressures, microhardness and roughness. The results allow to mainly conclude that thermal resistance dependency on mounting pressure is negligible for small values of roughness and microhardness as well as smaller values of these parameters allow to reduce the thermal resistance. It was also observed that this field of research still has space to grow, specially in terms of random processes simulations and the studies of the phenomenon in new materials. The model's accuracy and uncertainty, as well of its sensibility to random error were analysed through statistical simulations.*

Keywords: *thermal contact conductance, microgap conductance, microhardness*

1. INTRODUCTION

The thermal contact resistance is a well-known phenomenon, concerning the resistance of a solid interface to the transfer of heat. Roughness in the surfaces of the solids, even when it appears perfectly smooth, reflects on the real area of contact between the specimens, assuring that it is considerably smaller than the nominal area. That is, the passage of heat through the interface is not only a conduction phenomenon, including convection and radiation through the interstices that are formed by the junction.

In the case of a thermal resistance circuit, this is translated to a finite difference in the temperature between points immediately close to the interface, given a specified heat flux through it. Thermal systems with more than one piece have then to be designed taking this into consideration, especially when the values of heat flow are very high; for instance, the heat control in cryogenic systems and in nuclear reactors, where the temperature differences are of importance in the security of operations.

Research regarding the Thermal Contact Resistance (TCR) had not developed a theoretic analysis until 1963, being, prior to that, focused only in experimental investigations. A work by Thomas and Probert made a survey of the experimental data, concerning interfaces of copper and aluminium alloys, as well as stainless steels and miscellaneous materials (Yovanovich, 2005).

Through the years 1940-1955, many technical reports were produced for studies in the aircraft industry, concerning experimental correlations. From 1950-1970, nuclear industries produced an effort by countries like the USA, Canada, France and Russia to get a better understanding of the phenomenon. These studies focused on instances with high temperature, high mechanical pressures, and, especially, high gas temperature, for tertiary fissions in a nuclear reactor generate helium-4 and tritium. These applications required a deep understanding of gas kinetics, as well as intricate relationships between the gases and the solids encapsulating them (Yovanovich, 2005).

From 1960 to 1985, NASA started studying the phenomenon for applications with spacecraft, regarding the use of interstitial foils made of tin, lead and indium. From 1970 until now, the main concern about TCR is in the industry of microelectronics, particularly microprocessors, in search for an efficient way of maintaining a low enough temperature that wouldn't damage the circuits, due to their intense dissipation of energy during calculations. These studies focused on the creation of efficient interstitial fluids, the so-called TIMs (Thermal Interface Materials), generating a myriad of thermal grease technologies, which are generally composites containing particulate fillers such as aluminium and magnesium oxides, boron nitrite and diamond powder. There are also phase change materials, that are assembled in the solid form,

changing to the grease form during application, as well as adhesives and glues.(Yovanovich, 2005)

This work aims to have a deep understanding of a theoretical model produced for predicting the thermal contact resistance in a solid-solid interface. Such theoretical considerations are thoroughly examined hereafter.

2. THEORETICAL MODEL

The model chosen to be studied in this work was developed by M. G. Cooper, B.B. Mikic and M.M. Yovanovich, in a cooperation of the University of Cambridge in England, the Massachusetts Institute of Technology in the United States and the University of Poitier in France (Cooper *et al.*, 1969).

It is the first theoretical development concerning a great number of parameters, aiming to predict the thermal resistance based on the roughness profile, the application pressure and the microhardness of the materials.

The model's main idea is the appliaction of a single elemental contact analysis, introduced in 1968 by Mikic (Cooper *et al.*, 1969), that simplifies the problem considering its behaviour as two cylinders with pointed extremities that touch each other. The model then introduces a statistical integration of these elemental contacts in the whole junction area.

2.1 Single Contact and the Constriction Parameter

It is mathematically demonstrated (Cooper *et al.*, 1969) that the treatment of contact between symmetrical solids generates a plane in z=0 with constant temperature. This is an important result that allows to introduce the same boundary conditions to all contacts in a junction, thus making it possible to integrate their contributions without much error.(Cooper *et al.*, 1969)

The argument presents a junction between two symmetrical objects, such that their external boundary is perfectly matched, that is, the heat flux entering each point of the boundary leaves the system in the symmetrical opposite point in the other object. That is illustrated in Fig. 1

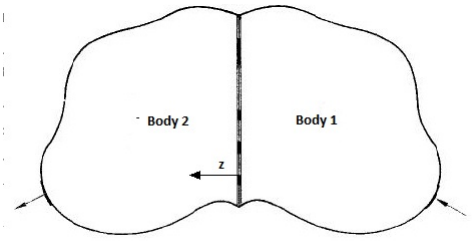

Figure 1: Representation of a symmetrical flow channel(Cooper *et al.*, 1969)

In a permanent state with no generation of heat, the temperature field is the solution of a Laplacian equation, $\nabla^2 T = 0$, in both bodies simultaneously. It is shown that a solution can be devised with specific boundary conditions on each of the bodies separately, in a way that the only difference in each temperature field is a sign symmetry. If we state that $T = 0$ where $z = 0$ in both problems, and devise the other boundary conditions in such a way that they merge at $z = 0$, the same solution can be found for both bodies, where $T(x_o, y_0, z) = -T(x_0, y_0, -z)$, and can be regarded as a solution to the whole problem by the theorem of existence and uniqueness of the solution of a homogeneous differential equation, differing only by a constant of integration. Thus, the symmetry guarantees that, at $z = 0$, that is, the section where the bodies make contact, has the same temperature in all its points, independently of the behaviour of the temperature field in other directions. The full argument can be understood in Cooper et al.(1969).

The contacts are then idealised as two cylinders of same radii, with pointed edges in their centres, which exchange heat trough an area of radius c, as shown in Fig. 2.

The geometry for solving the problem regarded the cylinders without pointed edge, representing that edge as a region in the boundary, thus solving it in the aspect of two conforming cylinders. Outside the real contact, $c < r < b$ the boundary is described as having no heat exchange.

For computation of the thermal contact conductance, h_c, the model regards a small disc situated in $z = 0$ with sufficient thickness to enclose the area where the heat constriction effects are translated as a difference in temperature, ΔT_c, between the surfaces of the bodies. The first relation is then given by Eq. 1;

$$Q = h_c \pi b^2 \Delta T_c \tag{1}$$

where h_c is the interface conductance, and ΔT_c is the temperature difference between the faces of the small contact disc, and b is the cylinder radius, as seen in FIg. 1. The model treats the boundary at z=0 as a mixed boundary condition, in which the temperature is constant in the area of contact, and the heat flux is null in the gap. This generates the boundary

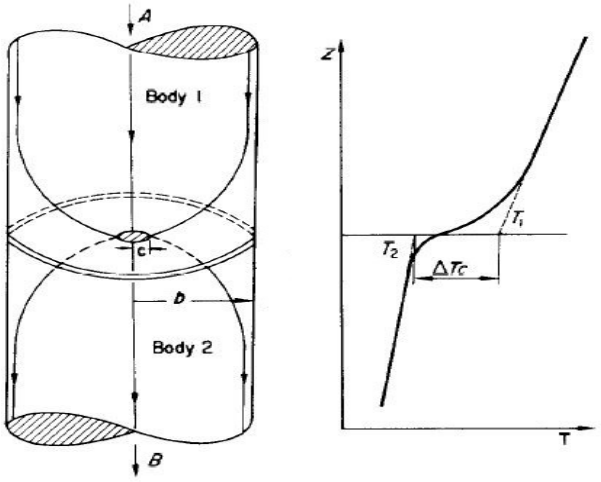

Figure 2: Representation of an elemental cylindrical flow model(Cooper *et al.*, 1969)

problem, with c as the contact region radius and k_1 as the thermal conductivity of body 1:

$$\begin{aligned}
&\nabla^2 T = 0 \\
&\left.\begin{aligned} k_1 T &= T_0,\ 0 < r < c \\ k_1 \frac{\partial T}{\partial z} &= 0,\ c < r < b \end{aligned}\right\} z = 0 \\
&k_1 \frac{\partial T}{\partial z} \to \frac{Q}{\pi b^2},\ \text{as } z \to \infty \\
&k_1 \frac{\partial T}{\partial r} = 0,\ r = b
\end{aligned} \tag{2}$$

This is a two-dimensional partial differential equation. The first difficulty is to transform the first two boundary conditions, which are a combination of constant heat flux and constant temperature, into a form where both are stated as a heat flux. This was accomplished by modelling of the first condition as a function, where the heat flux $\partial T/\partial z \propto 1/\sqrt{c^2 - r^2}$, which would attain an approximately constant temperature when r is small, representing a pointed edge. The details of the reasoning can be found in Cooper et all (1969).

Solving this problem in cylindrical coordinates, using the separation of variables technique, in which T is divided into two one-dimensional functions $T(z, r) = Z(z)R(r)$ gives place to a Bessel equation, as showed in Equation 3,

$$r^2 R'' + rR' + \alpha^2 r^2 R = 0 \tag{3}$$

where α is the eigenvalue assumed to be positive, obtained from the equation regarding the function for Z, as $Z''/Z = \alpha^2$. for which it is possible to obtain a solution that diminishes with z until the effects of the boundary are null at $z \to \infty$. This equation is solved by use of the Frobenius method, in which the solution is assumed to have the form $R = \sum_{n=0}^{\infty} A_n r^{m+n}$, then to be easily differentiated, as it is a polynomial. This assumed solution is then applied to the original equation, and after the sums are manipulated, and the indicial equations are analysed, the problems arrives to the solution in series form,

$$R(r) = \sum_{n=0}^{\infty} \frac{(-1)^n (\alpha r/2)^{2n}}{n!\Gamma(n+1)} = J_0(\alpha r) \tag{4}$$

J_0 is the know Bessel function of first kind and order 0 which has tabulated values calculated numerically. Given this result, the form of the solution of the system show in Eq. 2 is:

$$T(z, r) = \frac{Q}{\pi b^2} z + \sum_{n=0}^{\infty} C_n e^{-\alpha_n^2 z} J_0(\alpha_n r) + C_0 \tag{5}$$

where α_n are the eigenvalues, given that the solution is a sum of all possible infinite solutions, each with different α_n, by the principle of superposition. These eigenvalues are evaluated given the fourth boundary condition of System 2, which states that

$$J_1(\alpha_n b) = 0$$

,due to the differentiating properties of the Bessel function.

It is here that the the new boundary conditions for the pointed edge are introduced as substitutes for the first two conditions in Eq. 2:

$$\begin{aligned} k_1 \frac{\partial T}{\partial z} &= \frac{Q}{2\pi c\sqrt{c^2 - r^2}},\ 0 < r < c \\ k_1 \frac{\partial T}{\partial z} &= 0,\ c < r < b \end{aligned} \tag{6}$$

The C_n, coefficients of the infinite sum solution in Eq. 5 can be obtained by use of the orthogonal properties of the Bessel function, as well as the integral relationship,

$$\int_0^c \frac{rJ_0(\alpha r)}{\sqrt{c^2 - r^2}} dr = \frac{sin(\alpha c)}{\alpha} \tag{7}$$

It is then possible to apply the integrals to find the eigenfunctions of the solution with respect to each of the terms of the infinite sum, applied to the first boundary condition now modified by Eq. 6, in search for the eigenvalues. This gives:

$$\frac{Q}{\pi b^2} k_1 \int_0^c rJ_0(\alpha_n r)dr + C_n \alpha_n \int_0^b rJ_0^2(\alpha_n r)dr = \frac{Q}{2\pi k_1 c} \int_0^c \frac{rJ_0(\alpha_n r)}{\sqrt{c^2 - r^2}} dr \tag{8}$$

so that,

$$C_n \alpha_n \frac{b^2}{2} J_0^2(\alpha b) = \frac{Q}{2\pi k_1 c} \frac{sin(\alpha_n c)}{\alpha_n} \tag{9}$$

Thus, substituting the values for C_n in the theoretical solution (Eq. 5) we have its final form,

$$T = C_0 + \frac{Q}{\pi k_1 b^2} + \frac{Q}{\pi k_1 c} \sum_{n=1}^{\infty} e^{-\alpha_n z} \frac{sin(\alpha_n c) J_0(\alpha_n r)}{(\alpha_b)^2 J_0^2(\alpha_n b)} \tag{10}$$

The constant temperature condition can be recuperating by taking a mean value of the solution in $z = 0$, as shown in Eq. 11

$$T_0 = \frac{1}{\pi c^2} \int_0^c (T)_{z=0} 2\pi r dr = C_0 + \frac{Q}{4k_1 c} \psi(c/b) \tag{11}$$

where $\psi(c/b)$ is the *constriction parameter*, a fucntion of the cylinders radius b and the contact radius c, representing the resistance of the media on the constriction and spreading of the heat to fit through a small passage, as shown in Fig. 3. The expression for the parameter was then simplified for practical uses through a correlation, but its theoretical development is important to obtain other micro-geometric parameters to be devised in next section. Equation refeq:psi represents the theoretical and correlated relations for ψ:

$$\psi(c/b) = \frac{8}{\pi} \frac{b}{c} \sum_{n=1}^{\infty} \frac{sin(\alpha_n c) J_1(\alpha_n c)}{(\alpha_n b)^3 J_0^2(\alpha_n b)} = \left(1 - \sqrt{\frac{A_r}{A_n}}\right)^{1.5} \tag{12}$$

It is important to note that the last correlation is only possible if one considers no variation in the constriction parameter through all the contact points.

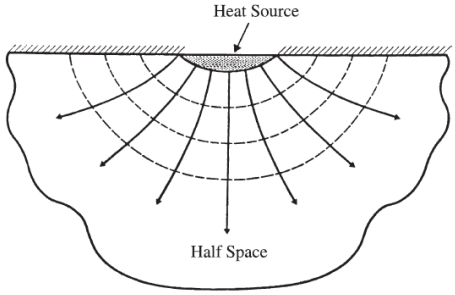

Figure 3: Representation of the spreading/constriction phenomenon. (Yovanovich and Marotta, 2003)

2.2 Multiple Contacts

From the previous equations its is then possible to develop a model for multiple points of contacts between the surfaces. It is understood that, if the nominal area (A_n) is thought as a division of small areas $A_{m1}, A_{m2}, ...A_{mn}$, which include each one contact point, then the heat can be seen as the sum of its contribution in each of these areas.

The fact that the contact temperature difference, ΔT_c must be equal for all contacts it translated into a relationship between the total heat and the heat in each contact. First, it gives it in an overall aspect:

$$\Delta T_c = \frac{Q}{2kc}\Psi\left(\frac{c}{b}\right) \tag{13}$$

Since ΔT_c must have a constant value, it is implied that the heat must be a weighted distribution, such as in Equation 14:

$$\frac{Q_1}{c_1/\psi_1} = \frac{Q_1}{c_1/\psi_1} = \frac{Q}{\sum_{j=1}^{m} c_j/\psi_j} \tag{14}$$

hence

$$Q_i = Q\frac{c_i/\psi_i}{\sum_{j=1}^{m} c_j/\psi_j} = Q\frac{c_i}{\sum_{j=1}^{m} c_j} \tag{15}$$

Considering no variation in ψ_i. This is then furthermore transformed into a relationship with the division of the area, since each individual area comprises one contact point:

$$A_{mi} = A_n\frac{Q}{Q_i} = A_n\frac{c_i/\psi_i}{\sum_{j=1}^{m} c_j/\psi_j} = A_n\frac{c_i}{\sum_{j=1}^{m} c_j} \tag{16}$$

This distribution of contacts is said to be "appropriate", but the term is not of high importance, since a non-appropriate distribution would be visible to the eye.

It is now possible to finally have the first equation regarding the thermal conductance of the junction, in terms of the distribution of contacts , the nominal area and the constriction parameter:

$$h_c = \frac{Q/A_n}{\Delta T_c} = \frac{1}{A_n}\sum\frac{Q_i}{\Delta T_c} = 2k\frac{\sum c_i}{A_n\psi} \tag{17}$$

2.3 Statistical Development

It is now understood from Equation 17 that the last step in obtaining the model is through an explicit expression capable of expressing the total area of contact by means of calculating the number of contact points and their respective radii. Having this information, it is possible to finally estimate the conductance of the junction.

The main difficulty is to determine the whole profile of the surfaces, since the instruments designed to generate profiles are only capable of measuring two-dimensional profiles of roughness. It is then necessary to estimate the number of contact points by means of incomplete information, such as a finite number of profiles obtained with a profile-meter, a measure of the roughness of the materials (a poorer information), or even the mere knowledge of the surfaces' finishing process.

Firstly, the junction of two complex profiles, as seen in Fig. 4a, was remodelled into a single equivalent profile, assuming that the softest material would suffer plastic deformation, therefore adjusting to the contact point without spreading its radius, as seen in Fig. 4b.

The argument used by the authors consists in dividing the apparent area by means of parallel traces, with a constant (very small) distance between them. The total length of all these lines lying in the apparent area of contact is $A_n\delta$. The length of the segment lying within each A_{ri} is then approximated by A_{ri}/δ. Then, for the average line, as the distance δ tends to zero, and the error in calculating their total lengths tends to zero, it is shown that:

$$\lim_{\delta\to 0}\frac{\sum A_{ri}/\delta}{A_n/\delta} = \frac{\sum l_c}{L} = \frac{A_r}{A_n} \tag{18}$$

By that, it is possible to estimate the real area of contact by means of calculating the average length of contact in a two-dimensional profile. This profile is now introduced as a random collection of heights, in which the probability of them touching is assumed to have a Gaussian distribution.

By designating a random variable as the sum of the heights of each one of the solids, it is possible to calculate the average length of of contact by means of a statistical integral of the probability of touching bodies in a two-dimensional roughness profile.

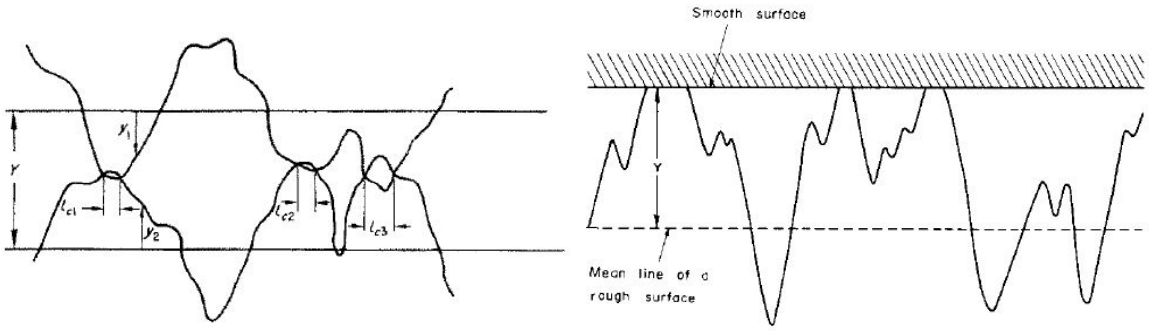

(a) (b)

Figure 4: Two profiles of a junction: (a) Representation of parameters Y,y_1, y_2,and l_c;(b) the equivalent profile for the model of pure plastic contact (Mikic, 1974)

The integration is set by the random variable $(y_1 + y_2)/\sigma = y/\sigma$, which is then considered to represent contact if it is higher than the roughness mean-planes separation, Y, normalised by the junction effective RMS roughness, σ, creating the $\lambda = Y/\sigma$ parameter. The normalisation is necessary to get an integral within the standard version of the distribution. The result is an estimation of the ratio of real area of contact to the nominal area of the junction. Figure 5 represents the integration, that is explicit by Equation 19:

$$\frac{A_r}{A_n} = \frac{\sum l_c}{L} = \left[1 - \int_0^{\lambda} \frac{1}{2\pi} e^{\frac{-(y/\sigma)^2}{2}}\right] / L \tag{19}$$

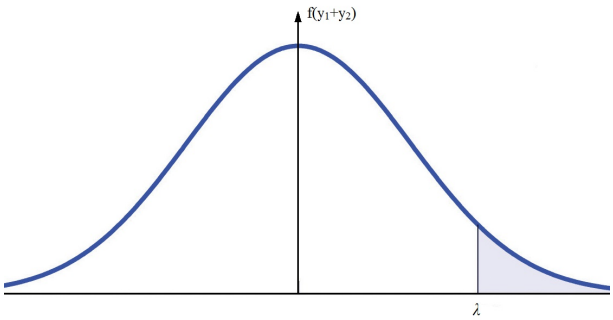

Figure 5: Representation of the statistical integration of the model

The evaluation of this integral establishes the first of three relations that assemble the micro-geometric properties of the junction. The real area of contact is finally predicted by Eq. 20,

$$\frac{A_r}{A_n} = \frac{1}{2}\text{cerf}(\frac{\lambda}{2}) \tag{20}$$

where cerf is the Complementary Error Function (Yovanovich, 2005).

Through use of the called method of counting functions, it is possible to relate the mean-slope s of the profiles, represented by a random process in the variable dy/dl, that is, the derivative of the peak heights, it was possible to devise a relationship between the mean slope and the number of contact points,

$$\frac{2\sigma\eta_c/L}{s} = \frac{e^{-\lambda^2/2}}{\sqrt{2\pi}} \tag{21}$$

$$\frac{\eta_c}{L}\frac{2\sigma}{s} = \text{mean}\left(\frac{\sum l_c}{L}\right) \tag{22}$$

thus resulting in the other two relations of the model, that explicit the said micro-geometric parameters of the junction: the total number of contact spots η_c; and the average contact spot radius c_c. Knowing the real area of contact is not sufficient

to predict the thermal contact conductance, for the effects of constriction would not be comprised in the calculations. Eqs. 23 and 24 are then (Yovanovich, 2005):

$$n_c = \frac{1}{16}\left(\frac{s}{\sigma}\right)^2 \frac{e^{-\lambda^2}}{\operatorname{cerf}(\lambda/\sqrt{2})} \tag{23}$$

$$\alpha_c = \sqrt{\frac{8}{\pi}}\left(\frac{\sigma}{s}\right) e^{\lambda^2/2} \operatorname{cerf}(\lambda/\sqrt{2}) \tag{24}$$

Through Eq. 20, it is necessary to assess the value of λ, in a reverse manner, as seen in Eq. 29:

$$\lambda = \sqrt{2}\operatorname{cerf}^{-}1\left(\frac{2A_r}{A_n}\right) \tag{25}$$

making it possible to compute the micro-contacts conductance,h_c through the main model equation, Eq. 28

$$h_c = \frac{2\eta_c \alpha_c k_{\text{eff}}}{\psi(A_r/A_n)} \tag{26}$$

where $k_{\text{eff}} = 2k_1k_2/(k_1 + k_2)$ is an effective juntion conductivity.

2.4 Deformation Analysis

It is sufficient to assume that the deformation would fall on a plastic region, since there was made Hertzian analysis which deduced the interference at which the elastic stresses are exceeded (Mikic and Rohsenow, 1966). The analysis indicated that, with roughness in dimensions of 10^{-4}, which are high, less than 1% of the area in contact is still in elastic regimen.

It is important to note that work hardening, creep, thermally induced distortion and other phenomena can have a significant effect on the characterisation of the deformation, so that the surfaces simulated should be assumed to be in first contact.

This gives space to the assumption that the mean pressure *under contacts* is simply the superior limit that can be applied until no deformation is possible, that is, the results of an indentation test, particularly the Vickers microhardness test. This microhardness has the convenience of being measured by application of an indenter of similar size that of the contacts, although some dimensions bigger. (Mikic, 1974)

That means that, applying a force balance, one can obtain a key relation between the applied pressure and the real area of contact, as seen in Eq. 27:

$$PA_n = H_v A_r \rightarrow \frac{P}{H_v} = \frac{A_r}{A_n} \tag{27}$$

This introduces the last parameter in the model, thus completing it, as it is now summarised in the few relations:

$$h_c = \frac{2\eta_c \alpha_c k_{\text{eff}}}{\psi(A_r/A_n)} \tag{28}$$

$$\lambda = \sqrt{2}\operatorname{cerf}^{-}1\left(\frac{2P}{H_v}\right) \tag{29}$$

$$\psi(c/b) = \left(1 - \sqrt{P/H_v}\right)^{1.5} \tag{30}$$

and Eqs. 23 and 24. It is noted that the Vickers microhardness applied to the model must be that of the softest material in the junction.

2.5 Microgap Conductance

The micro-gap conductance is directly related to the interstitial fluid physical state. The heat transfer through gases can be classified in four different regimens:

- Continuous regimen
- Temperature leap regimen
- Transition regimen

- Molecular Regimen

One convenient parameter to characterise the regimens is the Knudsen Number, defined as the ratio between the mean molecular free-path,Λ and a characteristic dimension of the problem L_c

$$\text{Kn} = \frac{\Lambda}{L_c} \tag{31}$$

In the continuous regimen (Kn $<< 1$), the heat transfer happens mainly through collisions between the gas molecules. The gas' thermal conductivity does not vary with pressure, but it does with temperature. Nevertheless, in the most rarefied regimens (Kn $>> 1$), collisions are negligible.

The mean free-path is given by Eq. 32:

$$\Lambda = \frac{\mu v_m}{P} \tag{32}$$

where v_m is the most probable molecular velocity according to gas kinetic theory,P is the pressure, ans μ is the viscosity in Pa.s.

v_m can be computed by Eq. 33:

$$v_m = \sqrt{\frac{2k_bT}{m}} \tag{33}$$

where $k_b = 1.38.10^{-23}$ J/K is Boltzmann constant and m the gas' molecular mass in kg.

This analysis is necessary for a better categorisation of the heat transfer, so it can be further used in the Yovanovich model for micro-gap conductance.

In this model, the most important parameter regarding the gas' regimen is the *rarefaction parameter*, M. It is defined through Eq. 34 as the product of three other gas parameters: α_g represents the effects of gas-solid interactions, being specifically determined for each material involved in the junction, and depends both on the temperature and molecular mass of the solid and the gas(Eq. 35); β_g represents physical properties of the gas in terms of the Prandtl number and the ratio $\gamma_g = c_p/c_v$ of its specific heats in constant pressure and constant volume, respectively (Eq. 36); Λ is the mean molecular free-path, which depends on temperature and molecular mass.

$$M = \alpha_g \beta_g \Lambda \tag{34}$$

$$\alpha_{g-s} = \frac{2 - \alpha_{g1}}{\alpha_{g1}} + \frac{2 - \alpha_{g2}}{\alpha_{g2}} \tag{35}$$

$$\beta_g = \frac{2\gamma_g}{\gamma_g + 1}\frac{1}{Pr} \tag{36}$$

In Eq. 35, α_{g1} e α_{g2} are the *thermal accommodation coefficients* of the gas-solid pairs in each of the two surfaces of the junction. They are defined as a kind of elastic coefficient, where one measures the temperature difference a molecule of gas suffers after reflecting in the solid's surface of temperature T_s

$$\alpha_g = \frac{T_r - T_i}{T_s - T_i} \tag{37}$$

where T_i is the gas temperature before the collision and T_r is its temperature after the reflection.

This temperature difference is defined for perfectly clean surfaces, that is, with no impurities retained in the solid. As it is frequently observed, solid-gas interactions shows an adsorption behaviour, and the gas molecules are retained in the solid surface. That turns the theoretical determination of the thermal accommodation coefficients a complex problem. To determine these coefficients in absence of impurity, it is necessary to devise an experimental process where the solid surfaces are treated in a high temperature vacuum (2000 to 4000K), thus extracting the impurities. That is the reason that only solid with high fusion point, such as tungsten, could be effectively tested. (Song, 1987).

Data for the accommodation coefficients prone to impurity effects were determined empirically for various solid-gas combinations.(Song, 1987).

The earliest model that predicted the micro-gap conductance was developed in the 1950's decade and assumes that the micro-gap can be represented as two parallel plates separated by an effective gap thickness δ. The conductance h_l was modelled as $h_l = k_l/\delta$. δ is estimated by correlations in therms of the superficial roughness, mainly the R_a (first moment).

When the physical size of the gas layer is comparable to the level of molecular movement of the gas, the continuum hypothesis is no longer valid. This effect is commonly called heat transfer in rarefied gas.. To analyse the effect, firstly it is studies using the Knudsen number.

Knudsen number is a parameter that characterises the heat transfer regimen, and is defined as

$$\text{Kn} = \frac{\Lambda}{d} \tag{38}$$

where Λ is the mean molecular free-path of the substance and d is the distance separating the plates.

Many authors decide to statistically correlate the distribution of roughness peaks. Yovanovich developed the model, again assuming a Gaussian distribution, and maintained it in the integral form. This model is called YIGC (Yovanovich Integral Gap Conductance), and takes the dimensional difference of the microgaps into consideration.

Thus, the model unites, through a statistical integral, the different conductances exhibited for micro-gaps of different dimensions, in parallel.

$$h_l = \frac{k_g}{\sigma}\sqrt{\frac{2}{\pi}}\int_0^3 \frac{\exp\left[\frac{-(\lambda+u^2)^2}{2}\right]}{u^2 + M/\sigma} u du = \frac{k_g}{\sigma} I_g \tag{39}$$

where u is an auxiliary variable, M is the rarefaction parameter, k_g is the thermal conductivity, λ is, again, the mean relative distance between the roughness mean-planes, and σ is the effective roughness of the junction.

The integral was simplified into a parameter I_g(Eq. 40):

$$I_g = \frac{f_g}{\lambda + M/\sigma} \tag{40}$$

and the auxiliary function f_g:

$$\begin{aligned} f_g &= 1 + 0.06(\sigma/M)^{0.8} \qquad \text{for} \qquad M/\sigma >= 1 \\ f_g &= 1.063 + 0.0471(4-\lambda)^{1.68}(\ln(\sigma/M))^{0.84} \qquad \text{for} \qquad 0.01 <= M/\sigma < 1 \end{aligned} \tag{41}$$

The model is based on the idea that the mean roughness plane distance, Y, previously computed through a force-analysis in the interface, would have its value corrected by the effects of rarefaction, as stated Eq. 42:

$$Y_c = Y + M \tag{42}$$

where Y_c is the corrected mean-plane relative distance.

In the model, the proposition was to comprise the effects of all the four different regimens of heat transfer through gas. For the transfer in continuous media, the M parameter is negligible, and has a higher contribution as the Knudsen number rises, augmenting the contact resistance.

When using a thermal interface material such as a thermal grease, the rarefaction effect is negligible. In that case, the statistical integral was further simplified by use of an auxiliary function, $f_{\text{continuum}}$, for reference

$$f_{\text{continuum}} = \frac{k_g}{h_l Y} = 1 + \frac{0.304}{\lambda} - \frac{2.29}{\lambda^2} \tag{43}$$

The whole model can then be computed through a sum of the micro-contacts and micro gap.

3. SIMULATIONS AND ANALYSIS

The simulations were carried on in Scilab open source software (ESI Group, 2019). Three sets of parameter testing, as well as an uncertainty analysis, a sensibility analysis, and a final comparative simulation were deemed sufficient to have a better assessment of the model's value and limitations. A final simulation was made to compute a specific situation of practical interest. Several adjustments had to be made to ensure the parameters' order of magnitude were appropriate.

3.1 Parameter analysis

The first two tests were made with the set of parameters used in a previous work, as stated in Yovanovich (1981). The first test studies the effects of the surface's effective roughness in the behaviour of the thermal contact conductance. The second studies the effects of microhardness, but still assuming that the accommodation coefficients are of similar behaviour. Tables 1 2 give the parameter values for the first and second test, respectively.

Figure 6 shows the first two parameter tests. At low mechanical pressures, the thermal contact resistance has higher sensitivity to these parameters. In a design scenario with fragile components, such as microelectronic devices or high-precision automated machinery, it is of vital importance to polish the surfaces of the cooler heat sinks and to choose softer materials for the heat exchange. In terms of contribution to the heat exchange, applications with high hardness materials can generate junction temperature drops (ΔT_c) of one Kelvin for each 5 W of energy flowing through it. This means that an average powered microprocessor can generate a temperature drop of over 15K in normal pressure applications.

Figure 7 shows a comparison between a junction with air as interstitial fluid, and another with two different thermal greases (thermal conductivity $k_{1g} = 2W/m^2.K$ and $k_{2g} = 11W/m^2.K$). The use of thermal grease greatly reduces the contact resistance, since its conductivity is three orders of magnitude higher than that of air.

Table 1: Parameters for first test - Junction of Stainless Steel 416 (Yovanovich, 1981).

Parameter	Adopted Value
k_{eff}	25.27 W/mÂš.K
M	0.081
H_c	2.59 GPa
k_g	0.0298 $W/m^2.K$
σ	$[0, 1, 2, 3, 4, 5, 10, 20]$ μm
m	0.130 deg

Table 2: Parameters for second test(Yovanovich, 1981).

Parameter	Adopted Value
k_{eff}	25.27 $W/m^2.K$
M	0.081
H_c	$[[0.2, 1, 5, 10, 50, 100, 200]$ GPa
k_g	0.0298 $W/m^2.K$
σ	4.11 μm
m	0.130 deg

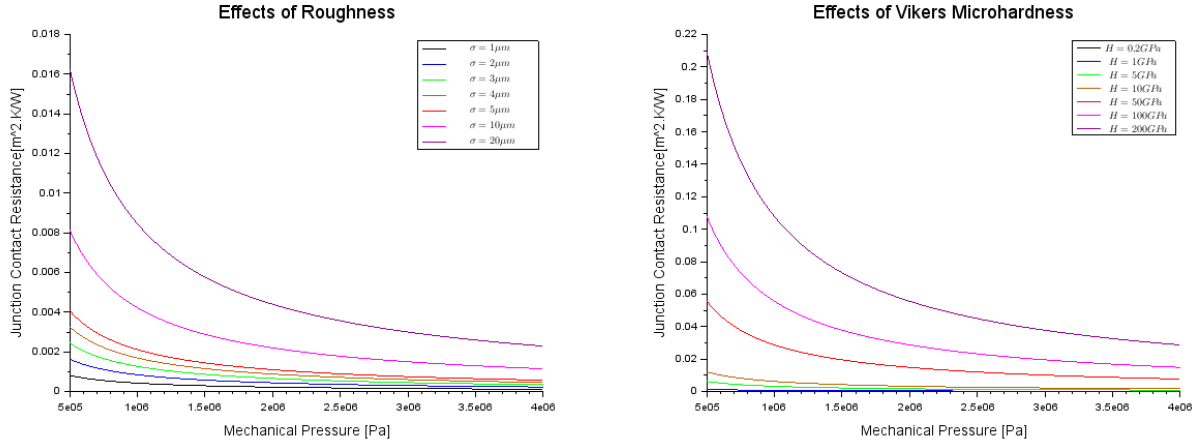

(a) (b)

Figure 6: Seven curves of the thermal contact resistance for (a) Different constant roughnesses; (b) Different constant Vickers microhardnesses

3.2 Uncertainty and Sensibility Analysis

A Monte Carlo simulation was programmed, assuming again that the random error in a hypothetical measurement of each parameter is given with a normal distributed random process. Its results vary in terms of the sensibility of the measuring instruments. The simulation attended to the procedures defined in (BIPM, 2008). Figure 8 illustrates a histogram of one possible outcome of the simulations. The final distribution mean and variance are used to assign the propagated error.

The sensitivity analysis was implemented to understand which parameters must be best controlled to reduce experimental error. The analysis method is based in the Sobol indices, which estimate the fraction of the final variance comes from each parameter, thus making it possible to assess the precision level needed for each parameter(Sobol, 2003)(Saltelli *et al.*, 2010).

Table 3 show the final Sobol indices for each parameter. This simulation was somewhat unsuccessful, since there was a great magnitude band between the parameters, from the microhardness measured in gigapascals to the roughness measured in micrometers. The original technique predicts a random process within the unit hypercube, a fact that greatly limits the flexibility for magnitude order adjustments. This resulted in an unseemly low index for some of the parameters, especially those of natural magnitude. A different technique for sensitivity analysis with a more appropriate magnitude management should be used.

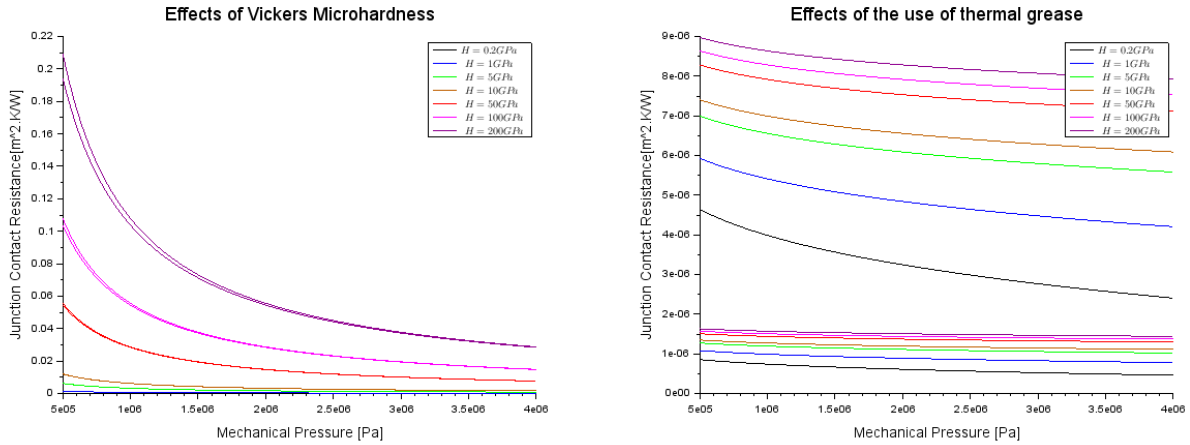

(a) (b)

Figure 7: Curves of Mounting Pressure x Contact Resistance. The lower curve in each pair of curves in same colour represents the effects of air as interstitial fluid. (a) Seven curves of constant Vickers Microhardness; (b) Curves with use of thermal grease. The highest family of curves represents a $2W/m^2.K$ grease, and the lowest, the $11W/m^2.K$

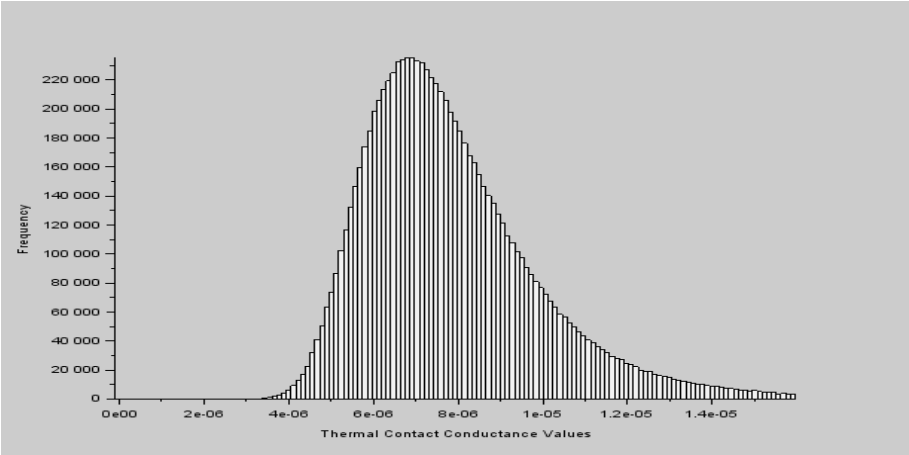

Figure 8: Histogram from the Monte-Carlo Simulation

Table 3: Sobol indices calculated by simulation

Parameter	Sobol Index
Pressure (P)	0.0088
Vickers Microhardness (H)	0.0097
Mean slope of asperity (s)	$8.27e^{-13}$
Effective Roughness (σ)	0.530
Conductivities ($k_{1,2}$)	$1.5e^{-12}$
Conductivity of fluid (k_g)	0.35
Rarefaction Parameter (M)	$1.39e^{-4}$

3.3 Comparative Simulation

A final comparative simulation was executed to assess the model's accuracy. The data was taken from a short communication from Turkey (Yüncü, 2006). Figure 9 shows the results. According to Yüncü, the data was taken from a vacuum environment. Dimensionless parameters were used to compare the data with a single curve, since each experimental point from the data had different parameters.

This is fair agreement, since it is a complex problem, revolving around random processes and microscopic properties. However, it shows possibility of a systematic error.

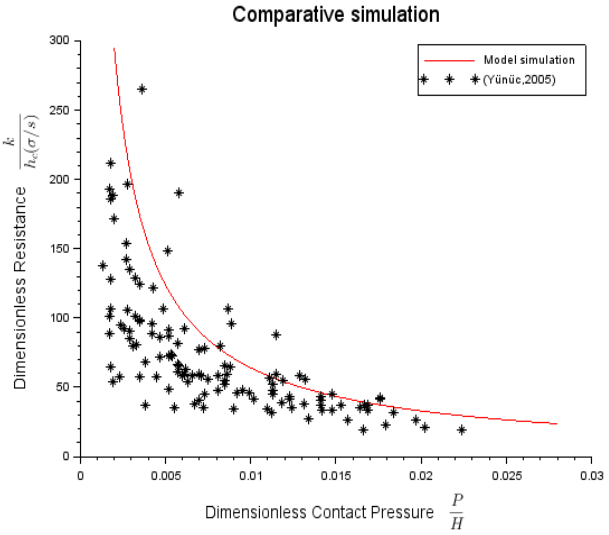

Figure 9: Comparative Dimensionless Simulation against experimental data

4. CONCLUSIONS

Although a complex problem with a great array of parameters, as well as a complex mathematical development involving random processes and irregular geometries, this is a well known model with fair agreement. The most limiting factor in reaching high accuracy is the difficulty of having available experimental data with convenient conditions. Some parameters, like the thermal accommodation coefficients, compromise the accuracy of the model because of their highly sensible character. Comparison with experimental data shows the possibility of systematic error.

Results show that the thermal contact conductance has higher sensitivity to roughness and Vickers microhardness when under low applied pressures. In short, the more delicate the application, the more important is to use soft and polished pieces. Higher mechanical pressures allow for lower effort un piece surface finish.

Uncertainty analysis by a Monte Carlo simulation revealed a tendency of overestimation the thermal conduction, thus underestimating the thermal contact resistance. The example results show possibility of near 50% errors. However, the sensitivity analysis revealed that the roughness and the gas thermal conductivity in the interstices are the greatest sources of error, indicating that a thorough control of the experimental measures for these parameters can be of high value in managing the accuracy of the model validation.

It is a great field for further research, especially in terms of random processes and simulations, having now the possibility of higher accuracy simulations by generating random geometry, instead of the analytic approach, which has aged. The directional problem, regarding biased distributions of roughness peak heights, could be better handled. Experimental data is scarce, leaving space for further experiments with modern materials, like highly conductive ceramics and composites.

5. REFERENCES

BIPM, 2008. “Evaluation of measurement data - supplement 1 to the "guide to the expression of uncertainty in measurement" - propagation of distributions using a monte carlo method”. Vol. JCGM 101:2008.

Cooper, M.G., Mikic, B. and Yovanovich, M., 1969. “Thermal contact conductance”. *International Journal of Heat and Mass Transfer*, Vol. 12, pp. 279–300.

ESI Group, 2019. “Scilab. version 6.0.2”. URL `https://www.scilab.org/`.

Mikic, B.B., 1974. “Thermal contact conductance: Theoretical considerations”. *International Journal of Heat and Mass Transfer*, Vol. 17, pp. 205–214.

Mikic, B. and Rohsenow, W., 1966. “Thermal contact resistance”. Technical Report 4542-41, National Aeronautics and Space Administration.

Saltelli, A., Annoni, P., Azzini, I., Campolongo, F., Ratto, M. and Tarantola, S., 2010. “Variance based sensitivity analysis of model output. design and estimator for the total sensitivity index”. *Computer Physics Communications*, Vol. 181, pp. 259–270.

Sobol, I.M., 2003. “Theorems and examples on high dimensional model representation”. *Reliability Engineering and System Safety*, Vol. 79, No. 2003, pp. 187–193.

Song, S., 1987. “Correlation of the thermal accomodation coefficient for engineering surfaces”. *University of Waterloo*.

Yovanovich, M.M., 1981. “New contact and gap conductance correlations for conforming rough surfaces”. *AIAA 16th*

Thermophysics Conference.
Yovanovich, M.M. and Marotta, E.E., 2003. *Heat Transfer Handbook, Chapter 4*. WILEY.
Yovanovich, M.M., 2005. "Four decades of research on thermal contact, gap, and joint resistance in microelectronics". *IEEE TRANSACTIONS ON COMPONENTS AND PACKAGING TECHNOLOGIES*, Vol. 28, No. 2.
Yüncü, H., 2006. "Thermal contact conductance of nominally flat surfaces". *Heat Mass Transfer*, Vol. 45.

6. RESPONSIBILITY NOTICE

The authors are the only responsible for the printed material included in this paper.